

Investigation of Critical Heat Flux Enhancement for Porous and Non-porous Structures without Surface Wettability Improvement

Han Seo, In Cheol Bang*

School of Mechanical and Nuclear Engineering

Ulsan National Institute of Science and Technology (UNIST)

UNIST-gil 50, Eonyang-eup, Ulju-gun, Ulsan Metropolitan City 689-798, Republic of Korea

*Corresponding author: icbang@unist.ac.kr

1. Introduction

Research on boiling heat transfer (BHT) mechanisms has been widely conducted because nucleate boiling is an effective mode of heat transfer up to the critical heat flux (CHF), which is the upper limit of the phase-change nucleate boiling. Nanoparticles and nano-sheets have been used in base fluids to enhance the BHT and CHF. Nanoparticles such as Al_2O_3 , TiO_2 , ZnO , Ag, Au and SiC have been studied for investigating the enhancement in the BHT and CHF. Most of the studies illustrated the enhancement in the heat transfer and CHF based on nanoparticle deposition during boiling occurrences [1-3]. Research on nanotechnology in boiling experiments such as the deposition of particles on heating surfaces, nanowires, and thin film coatings laid on a substrate was investigated as point of effective heat transfer methods [4]. Further, the modification of the heating area using nanoparticles during boiling occurrence was studied using IR thermometry [5]. Most of studies reported that the improvement of surface wettability is one of the major parameter attributing the change of the CHF. A theoretical model to predict the CHF based on the dynamic receding contact angle, which includes surface-liquid interaction effects, was accommodated the change of surface wettability due to the deposition of nanoparticles [6]. Park et al. [7], however, reported the reverse results that the enhancement in the CHF could not be explained by the relation of the improved surface wettability. They focused on the change of hydrodynamic instability wavelength due to the deposition of nanoparticles and concluded that the change of instability wavelength could be considered as the CHF enhancement mechanism. Therefore, an experimental CHF study without the change of surface wettability should be conducted to define the parameters attributing to the CHF.

This paper presents a study on the enhancement BHT and CHF with porous and non-porous surfaces deposited on a bare indium tin oxide (ITO) surface using FC-72 refrigerant. Porous and non-porous structures were fabricated using silicon carbide (SiC) and graphene. Plasma enhanced chemical vapor deposition (PECVD) system was applied to deposit the SiC surface as non-porous structure and porous SiC-coated surface was manufactured by deposition of

nanoparticles. For graphene surface, rapid thermal annealing (RTA) method and nanoparticles of graphene oxide were used for non-porous and porous structure, respectively.

2. Experimental Setup

2.1 Pool Boiling Facility

The pool boiling facility is schematically illustrated in Fig. 1. There are two vessels; the experimental procedure is conducted in the inner vessel and the outer vessel has a role of blocking heat losses from the inner vessel to the ambient environment, creating a saturation state for the inner vessel during the experiment. The reflection mirror is located at the bottom of the inner vessel to pass the IR intensity to the IR thermometry. An SC7210 IR thermometry (FLIR systems) is used for characterizing the heater surface. The calibration of the IR intensity to the heater surface temperature is done via a thermocouple attached on the heater surface. The calibration progress is conducted for every heater surface. Using calibration process, the maximum error is less than 1%, 0.5 °C.

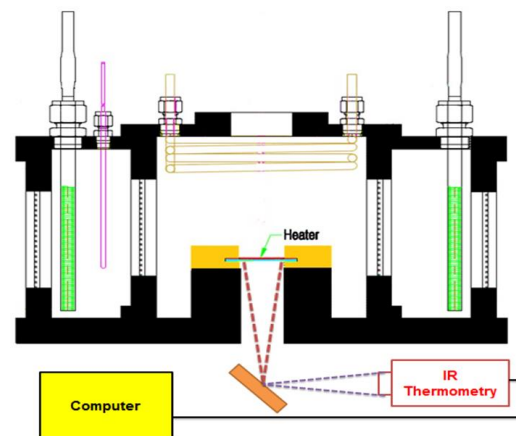


Fig. 1. Pool Boiling Facility

2.2 Preparation of Heater Surfaces

A sapphire glass with 1 mm thickness was used as the substrate material because it has high optical and high thermal transmissions. On the sapphire substrate, the ITO material was used as bare heater surface because

this material is optically transparent to visible wavelength and opaque at the IR spectrum. The material properties of the substrate and the bare ITO heating surface allowed the usage of the IR thermometry. The ITO layer is deposited on the sapphire substrate with the area of 50 mm × 32 mm. The average thickness of ITO layer is 750 nm. The silver busbars are printed at the end of the ITO surface with dimensions of 9 mm × 32 mm. Finally, the heating area of the bare ITO surface is 32 mm × 32 mm. The sheet resistance of the ITO layer is in the range 9–11 ohm/sq. Non-porous and porous surfaces using SiC and graphene were deposited on the bare ITO surface.

PECVD method was applied to make the non-porous structure of the SiC surface. PECVD system is operated in the low temperature compared to conventional CVD system so the bare ITO surface could be used in the PECVD system without the change of ITO characteristic. The average coating thickness of non-porous SiC surface is 3 μm. SiC porous structure was prepared with nucleate boiling using the SiC nanofluid. A 0.01 vol% SiC/water nanofluid was fabricated and boiled for 15 min at 632 kW/m² in the pool boiling facility to coat the nanoparticles on the bare ITO surface. The average porous coating thickness was 7.8 μm based on scanning electron microscopy (SEM) results.

For graphene surface, RTA method was applied to coat the non-porous graphene surface on the bare ITO. The formation of graphene layer was developed on a silicon (SiO₂/Si) wafer at 1000 °C during 5 minute in the rapid thermal annealing under vacuum condition. The non-porous graphene layer had 2~3 nm thickness based on the fabrication condition. Porous coating layer of graphene was prepared as the same method of the SiC porous structure. As shown in Fig. 2, non-porous and porous surfaces of the SiC and the graphene were confirmed using SEM.

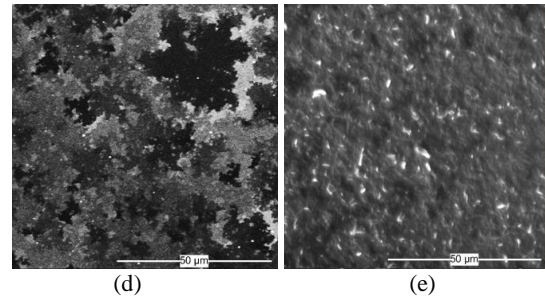
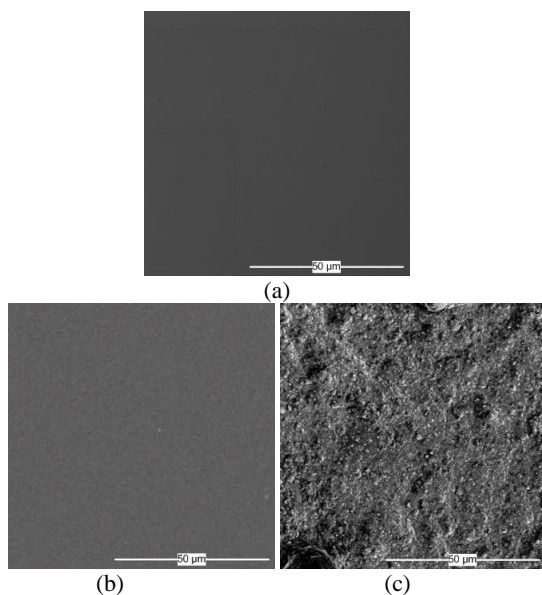


Fig. 2. SEM observation of heater surfaces: (a) bare ITO, (b) non-porous SiC, (c) porous SiC, (d) non-porous graphene, (e) porous graphene

3. Results and Discussions

In the experiment, the phenomenon of CHF was always generated with a sudden increase in the heater surface temperature. After the CHF is reached, the film boiling state can be observed if the heat flux is controlled; however the heater can burnout if the heat flux is not controlled. The heat flux from the heater surface was increased stepwise until the CHF was reached. When there was significant margin to reach the CHF, the heat flux increment was about 10 kW/m² per minute. Approaching the CHF, the heat flux increment was set at 1 kW/m². The CHF prediction value of FC-72 in the plate type surface was calculated as 148.15 kW/m² based on the hydrodynamic instability model [8]. In the present work, the average CHF value of the bare ITO surface was obtained as 120.8 kW/m². For SiC-coated surface, the values of CHF for the non-porous and the porous surface were increased by 15.7% and 58%. For graphene-coated surface, the CHF was increased by 9% for the non-porous surface and 89.9% for the porous surface.

Fig. 3 shows the boiling curves for the bare ITO, non-porous and porous surfaces of the SiC and the graphene. The experiment was conducted three times for each heater type and the boiling curves indicated the average experimental results. As shown in Fig. 3, the onset of nucleate boiling (ONB) for porous surfaces was triggered at low heat flux and low heat flux compared to the non-porous surfaces. This means that an effective BHT could be found in the porous structures, while non-porous coating surfaces did not show the BHT improvement compare to the bare ITO surface.

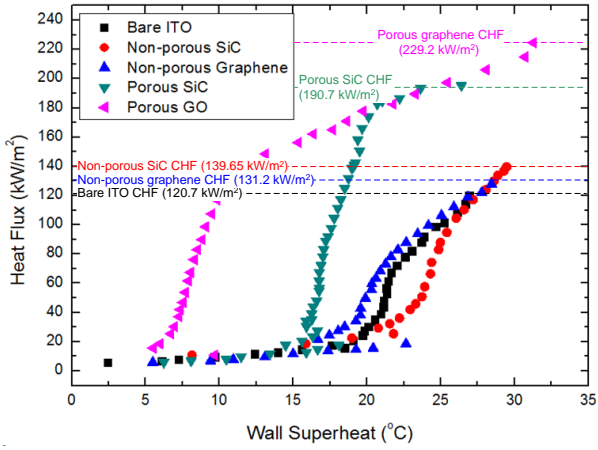


Fig. 3. Boiling curve for each heater surface

The enhanced BHT was observed in the porous surfaces, as shown in Fig. 3. All the heater surfaces showed hydrophilic condition with the working fluid (FC-72), which has low surface tension compared to water. Fig. 4 indicates static contact angle of each heater type. There were no differences in surface wettability even though different surface conditions were measured. The enhanced BHT can be attributed to the activation of microcavities of the heater surfaces. A large amount of microcavities can be activated and more bubbles are produced in the porous structures, leading to increase of heat transfer coefficient. Therefore, the enhancement in the BHT and the CHF was attributed to surface modification such as the formation of microporous structures.

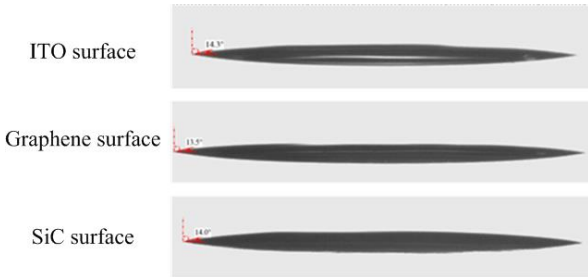


Fig. 4. Static contact angle measurements: ITO (14.3°), graphene (13.5°), SiC (14°)

As shown in Fig. 2, the surface characteristics changed from nanosmooth to porous structures owing to the graphene and SiC nanoparticles. According to the Liter and Kaviany model for porous structures in a pool boiling experiment, the porous structure can reduce the Rayleigh–Taylor wavelength, compared to a plain surface (bare ITO and non-porous SiC and graphene heaters). This porous layer can enhance the CHF according to the following equation [9].

$$q_{CHF}'' = \frac{\pi}{8} \Delta h_{fg} \left(\frac{\sigma \rho_g}{\lambda_m} \right)^{1/2} \quad (1)$$

where λ_m is the modulation wavelength. In this study, we supported this idea based on the CHF experiments by changing the surface characteristics using nanofluids. As shown in Fig. 2, porous structures for SiC and graphene were formed because of the deposition of nanoparticles. The average coating thickness of the porous SiC and the porous graphene surface were 7.88 μm and 1.9 μm , respectively. Therefore, the porous structure of the SiC heater can trigger the enhancement in the CHF.

Capillary pumping limit can be described as the other CHF enhancement mechanism. If the surface has porous structure with having characteristic diameter, the porous structure will provide a large capillary pumping force compared to the non-porous structure. Therefore, the porous structure could prevent the drying out of the heated surface and delay the CHF occurrence. The balance between the capillary force and the viscous-drag liquid limit can be found as [9],

$$\frac{q_{CHF,c}}{\varepsilon_s (\rho_l \sigma h_w / \mu_l) \left((K \varphi_s)^{1/2} / D \right)} = 1 - \frac{C_E D}{0.53 \varepsilon_s^2 \sqrt{\varphi_s}} \frac{q_{CHF,c}^2}{\rho_l \sigma h_w^2} \quad (2)$$

where K is permeability of the porous structure, D is the liquid flow distance, φ_s is the porosity of the structure, and C_E is the Ergun coefficient. Based on the SEM results, the value of characteristic diameter and the liquid flow distance (D) of porous SiC surface were measured as 0.2 μm and 9 μm , respectively. If the subarray porosity $\varphi_s = 0.47$ is assumed in the present study, the $q_{CHF,c}$ has 1705.6 kW/m^2 . The theoretical value of the capillary pumping CHF limit is higher than the experimental results. However, the capillary pumping supports the change of the CHF due to the porous structures.

4. Conclusions

In the present work the study of the BHT and CHF is conducted using non-porous and porous heater surfaces without the effect of surface wettability. The following conclusions are obtained.

(1) The average CHF value of the bare ITO surface was obtained as 120.8 kW/m^2 . For SiC-coated surface, the values of CHF for the non-porous and the porous surface were increased by 15.7% and 58%. For graphene-coated surface, the CHF was increased by 9% for the non-porous surface and 89.9 % for the porous surface. The CHF values of porous surface are higher than the CHF values of non-porous surface.

(2) There was no significant change in the surface wettability for the bare ITO, graphene, and SiC heater surfaces because FC-72 refrigerant which has low surface tension was used as the working fluid. It showed that the wettability is not the main surface parameter that is influencing in the BHT and CHF in this experiment.

(3) The porous structures can enhance the CHF based on the change of the modulation wavelength.

(4) The change of capillary pumping limit is one of the dominant CHF mechanisms in the work. The exact values of permeability and porosity should be considered based on the experiment.

REFERENCES

- [1] Bang, I.C., and Chang, S.H., Boiling Heat Transfer Performance and Phenomena of Al₂O₃-water Nano-fluids, *International Journal of Heat and Mass Transfer*, Vol. 48, 2407-2419 (2005).
- [2] Kim, S.J., Bang, I.C., Buongiorno, J., and Hu, L.W., Effects of Nanoparticle Deposition on Surface Wettability Influencing Boiling Heat Transfer in Nanofluids, *Applied Physics Letters*, Vol. 89, 153107 (2006).
- [3] Lee, S.W., Park, S.D., Kang, S., Kim, S.M., Seo, H., Lee, D.W., and Bang, I.C., Critical Heat Flux Enhancement in Flow Boiling of Al₂O₃ and SiC Nanofluids under Low Pressure and Low Flow Conditions, *Nuclear Engineering and Technology*, Vol. 44, 429-436 (2012).
- [4] Bang, I.C., and Jeong, J.H., Nanotechnology for Advanced Nuclear Thermal-Hydraulics and Safety: Boiling and Condensation, *Nuclear Engineering and Technology*, Vol. 43, 217-242 (2011).
- [5] Bang, I.C., Buongiorno, J., Hu, L.W., and Wang, H., Measurements of Key Pool Boiling Parameters in Nanofluids for Nuclear Applications, *Journal of Power and Energy Systems*, Vol. 2, 340-351 (2008).
- [6] S. G. Kandlikar, A Theoretical Model to Predict Pool Boiling CHF Incorporating Effects of Contact Angle and Orientation, *Journal of Heat Transfer*, 123 (6) (2001) 1071-1079.
- [7] S. D. Park, S. W. Lee, S. Kang, I. C. Bang, J. H. Kim, H. S. Shin, D. W. Lee, D. W. Lee, Effects of Nanofluids Containing Graphene/Graphene-oxide Nanosheets on Critical Heat Flux, *Applied Physics Letter.*, 97 (2006) 023103.
- [8] N. Zuber, Hydrodynamic Aspects of Boiling Heat Transfer, Ph.D. Thesis, Univ. of California, (1959).
- [9] Liter. C.S., Kaviany. M., Pool-boiling CHF Enhancement by Modulated Porous-layer Coating: Theory and Experiment, *International Journal of Heat and Mass Transfer*, Vol. 44, 4287-4311 (2001).